Available online at www.sciencedirect.com
SCIENCE DIRECT
Cement and Concrete Research 35 (2005) 1299–1304
Cement and Concrete Research

ITZ microstructure of concrete containing GGBS

J.M. Gao*, C.X. Qian, H.F. Liu, B. Wang, L. Li

Department of Materials Science and Engineering, Southeast University, Nanjing 210096, P.R. China

Received 12 March 2004; accepted 28 June 2004

Abstract

The interfacial transition zone (ITZ) of aggregate–cement paste and the morphology of hydrates in concrete containing ground granulated blast-furnace slag (GGBS) have been investigated using XRD, SEM and microhardness measurements. The experimental results demonstrated that GGBS significantly decreases both the quantity and the orientating arrangement of CH crystals at the ITZ. The CH crystal size becomes smaller because of the addition of GGBS. The weak ITZ between aggregate and cement paste was strengthened as a result of the pozzolanic reaction of GGBS. The above improvements become much more significant with the decrease of particle sizes of GGBS.

Keywords: X-ray diffraction; Microhardness; SEM; Interfacial transition zone (ITZ); Granulated blast-furnace slag

1. Introduction

Ground granulated blast-furnace slag (GGBS) is a glassy material from by-product of blast furnace ironmaking. It mainly contains calcium silicoaluminate with high reactivity [1]. GGBS can improve the fluidity of fresh concrete, reduce its bleeding ’and postpone the setting when Portland cement is partially replaced by GGBS in concrete. The early-age strength of the concrete with Portland cement partially replaced by GGBS is almost equal to that of the concrete before replacement while the strength at later ages is even much higher. Accordingly, its durability has been improved [2,3]. The introduction of GGBS has a great effect on the microstructure of concrete, which includes the interfacial transition zone (ITZ) between aggregates and the hardened bulk cement paste. The ITZ is a weakness zone in the microstructure of concrete, but it is one of the most important factors influencing the performance of concrete. The existence of a water-membrane and pores at the ITZ of aggregates results in a much more open microstructure and a high orientation of CH crystals in the zone.

The past research on the concrete containing GGBS has been conducted mainly on the macroscopic level. But they did not reach to the microstructure level. In this paper, the ITZ of aggregate–cement paste is studied together with the content and orientation of CH in this zone. The influence of particle size and the content of GGBS on the ITZ will also be discussed. Two specific surface area values, 425 and 600 m^2/kg, and several amounts of GGBS addition are involved. A kind of fly ash (FA) is adopted for comparison purpose.

2. Experiment

2.1. Materials

The chemical compositions of the cement, GGBS and FA are given in Table 1. Their specific surface area values are indicated in Table 2. In addition, a crushed basalt rock was used as coarse aggregate. Their particle sizes were in the range of 5–31.5 mm; a naphthalene superplasticizer was used in this experiment.

Figs. 1 and 2, respectively, show the particle morphology of GGBS with specific surface area 600 and 425 m^2/kg. Fig. 3 presents the morphology of FA used in this work.

* Corresponding author. Tel.: +86 25 8379 5618.
E-mail address: jmgao@seu.edu.cn (J.M. Gao).

0008-8846/$ - see front matter
doi:10.1016/j.cemconres.2004.06.042

Table 1
Chemical composition (%) of the cement, GGBS and FA

Component	LOI[a]	Insoluble SiO_2 in HCl		Al_2O_3	Fe_2O_3	CaO	MgO	SO_3	Na_2O	K_2O	Total
Cement	1.15	0.38	21.29	5.15	3.23	64.04	0.95	2.10	0.08	0.50	98.87
GGBS	–	–	32.4	16.21	0.34	36.35	9.59	1.78	1.27	0.56	99.18
FA	2.01	–	50.99	31.34	5.93	3.9	1.27	1.45	0.19	1.5	98.58

[a] Loss on ignition.

Micrographs were obtained by means of JSM-6300 Scanning Electronic Microscopy.

2.2. Specimen fabrication

The specimens for microstructure analysis were cast in 40×40×160 mm moulds. They were taken out from a curing room and broken into proper size pieces at selected times. Broken pieces were kept in pure alcohol to stop hydration. Before the SEM examination, the broken pieces were ground until the size of all the particles was less than 10 μm. The X-ray diffraction scanning range was 10–70°.

The specimens for ITZ microhardness test were cut into the 10-mm-thick slices. The test surface of the specimens containing the ITZ between aggregate and mortar was polished.

The specimens for ITZ morphology observation were cut into prisms of 8×8×5 mm. The ITZ should be at the centre of the specimens.

3. Experimental results and discussion

3.1. X-ray diffraction analysis

The self-hydration of cement and GGBS produces $Ca(OH)_2$. In a saturated solution of $Ca(OH)_2$, the pozzolanic reaction of GGBS consumes $Ca(OH)_2$. Therefore, the quantity of $Ca(OH)_2$ crystals depends on its formation and reaction rates in a $Ca(OH)_2$ saturated solution. When the formation rate is faster than the reaction rate, the amount of $Ca(OH)_2$ crystal increases and the height of the XRD peak increases. Contrarily, the peak is low. Fig. 4 is an XRD diagram of paste containing GGBS of specific surface area 425 m^2/kg and a partial replacement of Portland cement at weight fraction 40%. The peak height in the XRD curve in Fig. 4 corresponding to $Ca(OH)_2$ increases when the self-hydration rate of cement and GGBS is much faster than the pozzolanic reaction rate of GGBS at 1 and 7 days. When the pozzolanic reaction rate of GGBS increases, also in Fig. 4, for curing age of 28 days, there is a small decrease in

Table 2
Specific surface area (m^2/kg) of the cement, GGBS and FA

	Specific surface area
Cement	361
GGBS (Slag 1)	425
GGBS (Slag 2)	600
FA	425

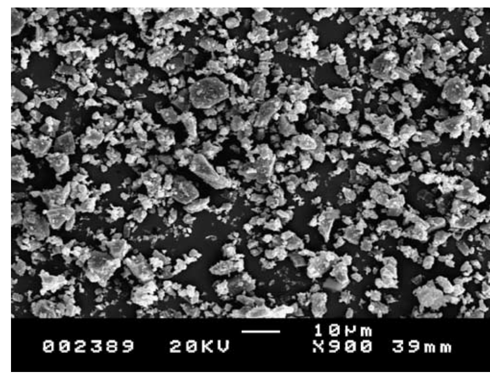

Fig. 1. GGBS of specific surface area 600 m^2/kg.

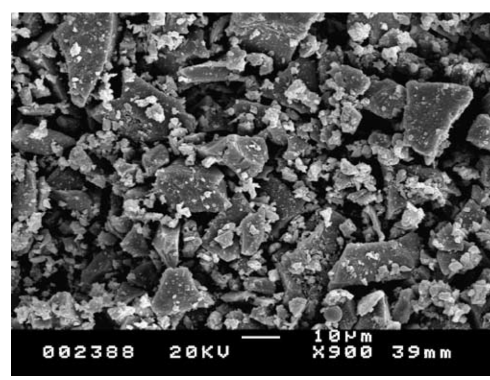

Fig. 2. GGBS of specific surface area 425m^2/kg.

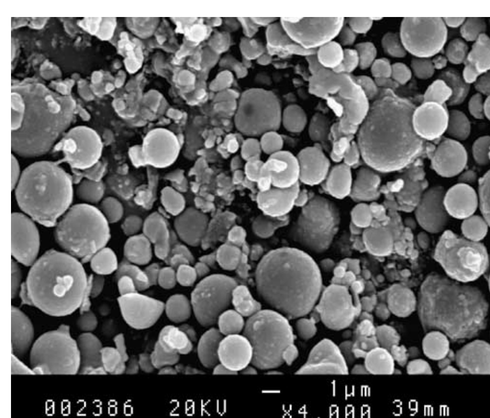

Fig. 3. FA of specific surface area 425m^2/kg.

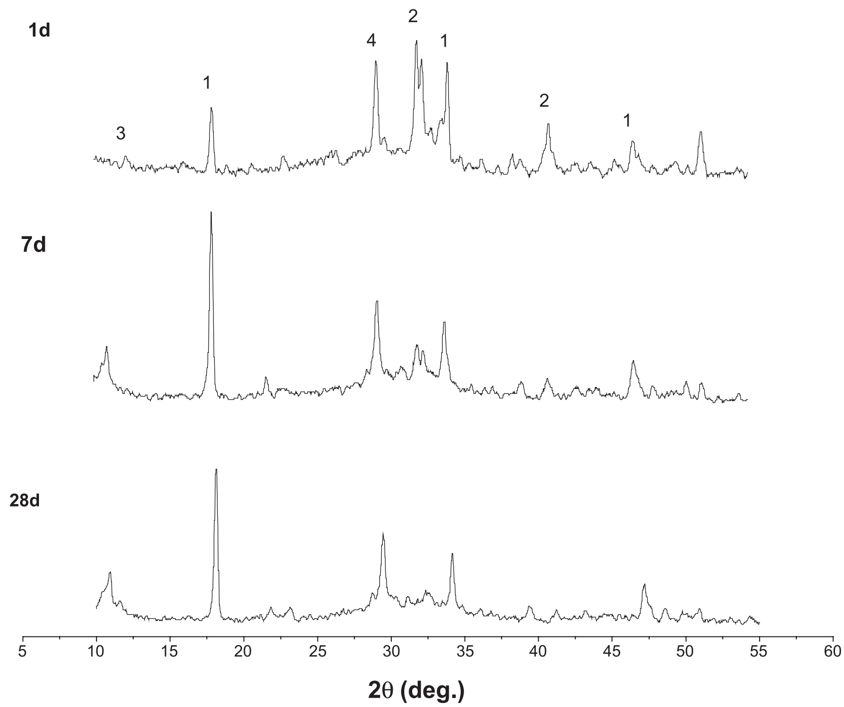

1——$Ca(OH)_2$ 2——C_3S, C_2S 3——C_4AH_{13} 4——C_3S

Fig. 4. XRD diagram of paste with GGBS (specific surface area 425 m^2/kg) replacing 40% Portland cement (weight fraction).

the $Ca(OH)_2$ crystal XRD peak height. The above analysis demonstrates that XRD diagrams can indicate the pozzolanic reaction rate of GGBS indirectly.

Fig. 5 is an XRD diagram of paste containing GGBS (specific surface area 600 m^2/kg) partially replacing Portland cement at a weight fraction of 40%. It is

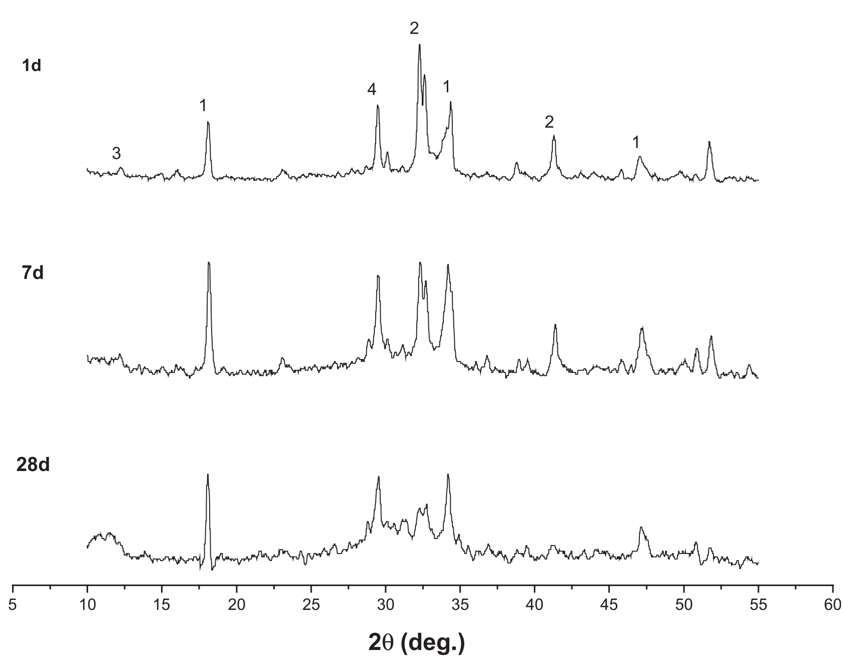

1——$Ca(OH)_2$ 2——C_3S, C_2S 3——C_4AH_{13} 4——C_3S

Fig. 5. XRD diagram of paste with GGBS (specific surface area 600 m^2/kg) replacing 40% Portland cement (weight fraction).

indicated in Fig. 5 that the CH peak height at 7 days is not as high as that in Fig. 4; this means that the pozzolanic reaction of GGBS in the sample starts to consume CH at 7 days. It means that the pozzolanic reaction of GGBS (specific surface area 600 m^2/kg and a weight fraction of 40%) starts earlier and proceeds at a fast rate.

3.2. Microhardness test of ITZ

Microhardness is a comprehensive parameter for various characteristics of ITZ [4]. Microhardness includes the information of mean crystal size, crystal orientation index of CH and pore microstructure. It is seen from Fig. 6 that there is a weak zone in the ITZ, which corresponds to low microhardness values (Hv). With partial substitution of GGBS for Portland cement, the 'valley' in the Hv distribution line disappears. In Fig. 6a, there is a very clear and good relation between the microhardness value and the substitution amount and the specific surface area of GGBS. The weak zone of the ITZ almost vanishes while Portland cement is partially replaced by GGBS (specific surface area 425 m^2/kg and a weight fraction of 40%). Also, at the same weight fraction, the weak zone of ITZ completely vanishes with the use of GGBS (specific surface area 600 m^2/kg). Moreover, the cementitious matrix is strengthened. The GGBS significantly decreases both the content and the orientating arrangement of $Ca(OH)_2$ crystals at ITZ. The fine GGBS particles produce a fast saturation balance of $Ca(OH)_2$; a small crystal size is obtained, which results in formation of a dense cementitious matrix. This also explains why the HPC of 40% Portland cement replaced by GGBS possesses an excellent resistance to freezing–thawing cycles. The weak zone of aggregation–mortar ITZ is also strengthened using a binary mixture of GGBS and FA to partially replace Portland cement (Fig. 6b). Compared with only GGBS partially replacing Portland cement, the enhancement effect of GGBS and FA simultaneously substituting for a part of Portland cement is less in the ITZ. The decreased enhancement effect corresponds to a small decline in microhardness value within a distance from the interface of 20 μm in the ITZ. It also explains why the strength of HPC with only GGBS replacing a part of Portland cement is higher than that with both GGBS and FA [5,6].

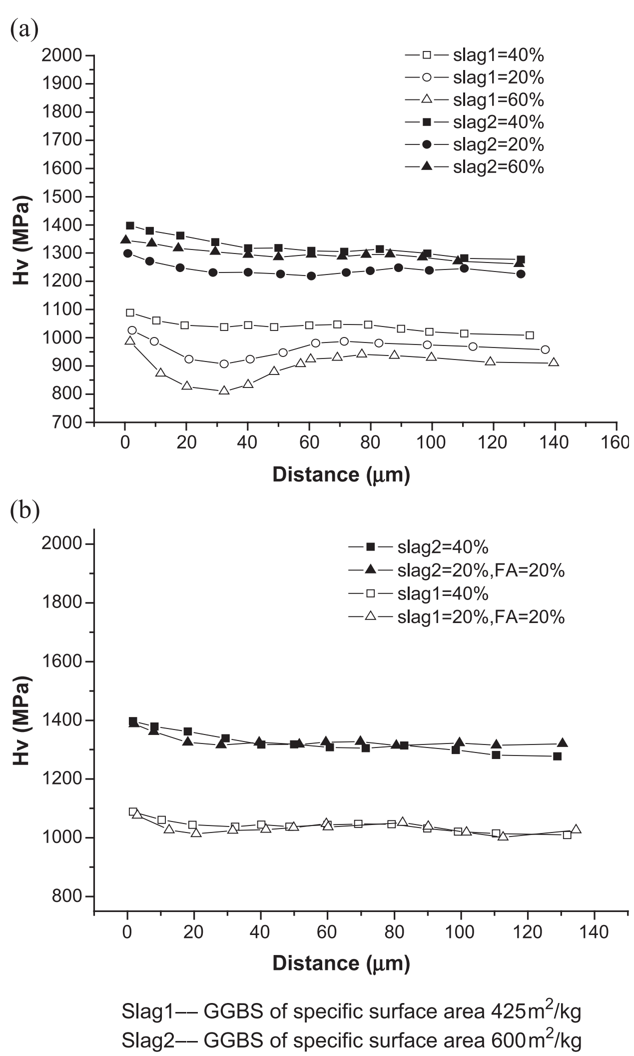

Fig. 6. Relationship of microhardness value for pastes containing GGBS and FA.

3.3. SEM test of aggregate–mortar ITZ

The ITZ morphology of HPC examined in the SEM varies with the different specific surface area and the weight fraction of GGBS. Fig. 7 contains the SEM pictures (×300 zoomed in) of aggregate–mortar ITZ at the curing age of 28 days. The study on SEM pattern of aggregation–mortar ITZ follows the regular results of the microhardness test. It is summarized as follows. At the same weight fraction of GGBS, the reaction products in the ITZ grow more compactly for the higher surface area material (compare Fig. 7b to a). At the same specific surface area of GGBS, the ITZ shown in Fig. 7a is much denser than the corresponding ITZ in Fig. 7d. The ITZ shown in Fig. 7d appears to be denser than that in Fig. 7c. It is apparent that GGBS at the weight fraction of 40% improves the ITZ microstructure at most.

$Ca(OH)_2$ crystals larger than 5 μm mean size are unable to be observed by SEM in HPC with GGBS partially replacing Portland cement as the aggregate–mortar ITZ is magnified ×10,000. Usually, the mean size of $Ca(OH)_2$ crystals is larger than 10 μm in conventional Portland cement concrete [7]. It demonstrates that the pozzolanic reaction of GGBS significantly decreases the mean size of the $Ca(OH)_2$ crystal before the curing age of 28 days in a hydrated Portland cement matrix. In Fig. 8, the mean size of $Ca(OH)_2$ crystals measured ranges from 3 to 4 μm.

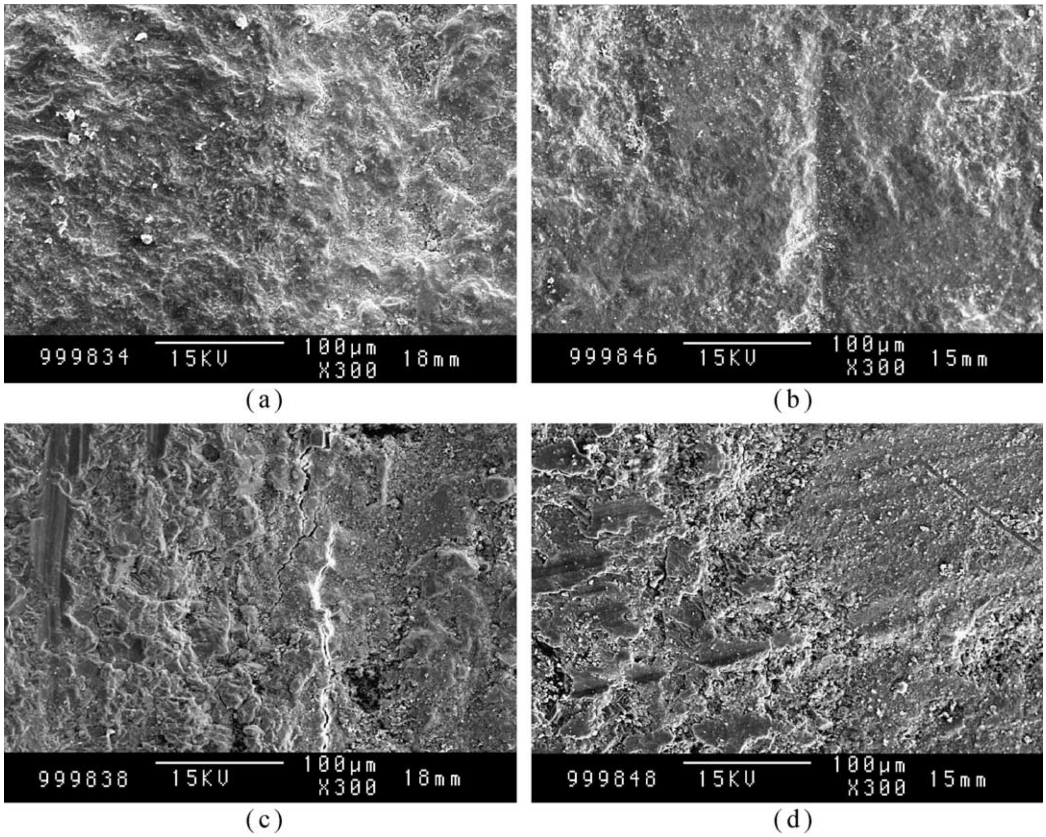

(a) weight fraction 40% and specific surface area 425m^2/kg of GGBS
(b) weight fraction 40% and specific surface area 600m^2/kg of GGBS
(c) weight fraction 20% and specific surface area 425m^2/kg of GGBS
(d) weight fraction 60% and specific surface area 425m^2/kg of GGBS

Fig. 7. Aggregate–mortar ITZ modality in HPC containing GGBS as a partial replacement Portland cement (The left side of the micrograph shows aggregates and the right presents cement paste).

3.4. Morphology of hydration product by SEM

The hydration degree and the morphology of the hydration products were also observed by SEM (see Fig. 9).

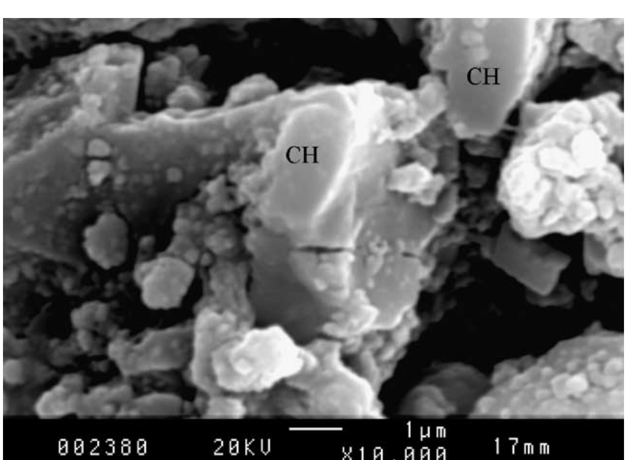

Fig. 8. $Ca(OH)_2$ crystal size in the SEM (×10,000 magnification).

A qualitative difference of reaction degree between GGBS and FA is evident in Fig. 9. At the curing age of 7 days, the GGBS particle surface is covered with hydration product, but the hydration product is not found on an FA particle surface until the curing age of 28 days.

The SEM picture also shows that there is no significant difference in the morphology of the reaction products between pure cement paste and a GGBS/(GGBS+FA)–cement paste.

4. Conclusions

- The pozzolanic reaction of GGBS starts at very early age. The reaction becomes more discernible at the curing ages of 7 to 28 days. The pozzolanic reaction rate is in direct proportion to the specific surface area of GGBS. These phenomena can be detected by XRD analysis and SEM observation.
- GGBS significantly decreases the content of $Ca(OH)_2$ crystals in the aggregate–mortar ITZ, as determined from XRD and SEM analysis. Moreover, it reduces the mean

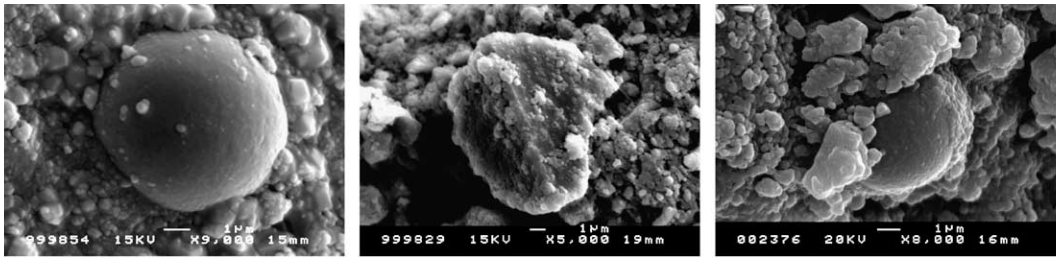

(a) (b) (c)

(a) Fly ash particle at curing age of 7d
(b) GGBS particle at curing age of 7d
(c) Fly ash particle at curing age of 28d

Fig. 9. SEM pictures of mineral addition of cement paste at different curing ages.

size of $Ca(OH)_2$ crystals, which make the microstructure of ITZ more dense; this can be observed by SEM. Due to these effects, high strength becomes possible for concrete with an optimum amount of GGBS replacing a part of Portland cement.

- The weak zone at the coarse aggregate–mortar interface almost vanishes in concrete in which 40% Portland cement is replaced by GGBS with a specific surface area of 425 m^2/kg. Furthermore, the weak zone completely vanishes when GGBS with a specific surface area of 600 m^2/kg replaces 20% of the Portland cement. Meanwhile, the cementitious matrix is strengthened. The test of microhardness shows these results.
- It is economical to partially substitute FA for GGBS. Both GGBS and FA simultaneous replacement of a part of Portland cement is effective in removing the weak aggregate–mortar ITZ.

References

[1] K. Ganesh Babu, V. Stree Rama Kumar, Efficiency of GGBS in concrete, Cem. Concr. Res. 30 (2000) 1031–1036.
[2] Feng Nai-Qian, High Performance Concrete, China Architecture and Building Press, Beijing, 1996, in Chinese.
[3] Tan Ke-Feng, Xin-Cheng Pu, Strengthening effects of FGFA, GGBS, and their combination, Cem. Concr. Res. 28 (12) (1998) 1819–1825.
[4] Zhao Guo-Fan, Peng Shao-Ming, Huang Chen-Kui, Structure of Concrete Containing Steel Fiber, China Architecture and Building Press, Beijing, 1999, in Chinese.
[5] Zhang Xiong, Wu Ke-Ru, Mechanism and key technology of GGBS. Dissertations About Research and Application of GGBS in Concrete, 2003, 1–8.
[6] Wang Bian, Gao Jian-Ming, Study on the strength and durability of concrete containing GGBS, China, Concr. Cem. Prod. 5 (2001) 7–9.
[7] V.S. Ramachandran, R.F. Feldman, J.J. Beaudoin, Concrete Science, China Architecture and Building Press, Beijing, 1981, in Chinese.